

# Influence of Water-Glass as an alkali activator on the microstructure and strength characteristics of Geopolymer Concrete

**M. Sowjanya Lakshmi<sup>1\*</sup>, Bollapragada Sessa Sreenivas<sup>2</sup>**

<sup>1</sup> Research Scholar, Department of Civil Engineering, KU College of Engineering & Technology, Kakatiya University Campus, Vidyananyapuri, Warangal, Telangana, India

<sup>2</sup> Professor, Department of Civil Engineering, KU College of Engineering & Technology, Kakatiya University Campus, Vidyananyapuri, Warangal, Telangana, India

Email: <sup>1</sup> sowsb2139@gmail.com, <sup>2</sup> bseshasreenivas@yahoo.co.in

## Abstract

This study investigates the influence of water glass as an alkali activator on the microstructure and strength characteristics of geopolymer concrete (GC). Ground granulated blast furnace slag (GGBS) and fly ash (FA) were used as binders, while water glass served as the alkaline activator. The research aimed to evaluate the physical properties of the materials, determine the mechanical properties of various GC grades (M25, M40, and M70), and analyze the GC microstructure using X-ray diffraction (XRD), energy-dispersive X-ray spectroscopy (EDS), and scanning electron microscopy (SEM). The workability of fresh GC was assessed using the slump test, while compressive strength, split tensile strength, and flexural strength were determined at 7 and 28 days. The results showed that increasing the alkali-to-binder ratio from 0.4 to 0.6 improved the mechanical strength parameters of GC for all mixtures. The highest compressive strengths of 28.3, 51.7, and 72.8 N/mm<sup>2</sup> were achieved by M25, M40, and M70 grades, respectively, with an alkali-to-binder ratio of 0.6 at 28 days of ambient curing. Microstructure analysis revealed a strong bond between the GGBS-based GC and the reacted FA at the interface, with the M70 grade exhibiting a denser and less porous structure. XRD analysis identified the crystalline phase of FA-GGBS-based GC, while EDS results showed that increasing Si content in M25, M40, and M70 grades led to higher strength and improved geopolymerization. The findings demonstrate the potential of GC as a sustainable alternative to conventional concrete, with water glass as an effective alkali activator for enhancing its mechanical properties and microstructure.

**Keywords:** Geopolymer, GGBS, Fly ash, Waterglass, Alkali-binder ratio, Mechanical Characteristics, Microstructure

## 1. Introduction

The industries that produce iron, steel, and electricity have significant industrial trash [1]. The production of waste from these sectors, like blast furnace slag and fly ash, has presented a difficulty for safe disposal [2]. Several investigations have been performed to address the issue of reusing or disposing of the trash produced by these sectors[3]. The result is that GC composite has become a material with enormous potential for using industrial waste to make concrete[4]. An environmentally friendly form of concrete that uses no cement is called GC[5,6]. An alkaline solution and aluminosilicates, such as GGBS & fly ash, are combined to create a geopolymer. Alkaline activation can help transform these aluminosilicates into a binder[5].

Davidovits developed the notion of geopolymer for the first time in 1978. According to his definition, geo

polymerization the poly-condensation process involving alumina-silicate source materials including metakaolin, fly ash, and rice husk ash produces an inorganic polymer that results in aluminosilicate frameworks in three dimensions [9]. Curing conditions significantly impact the geo-polymerization processes, and it has been shown that optimal curing conditions for GC are between 35°C and 85°C in temperature, with around 95% relative humidity [10]. As a result, different processing settings and their constituents impact entirely the final product's qualities[9].

In general, the strength and resistance of GC composites are similar to, or better than, those of environmental agencies[7,13]. Numerous studies have concluded that GC based on fly ash and GGBS are better resilient to acid and sulphate assaults [14,15]. The utilization of household and industrial waste as

aggregates in conventional and GC has been the subject of several research projects [3,6]. According to a few studies, GC composed of fly ash and GGBS has high weathering and chloride resistance [16,17]. According to the findings of several microstructural studies of geopolymer composites conducted using sophisticated tools and methods, including X-RD, FTIR, and SEM, GPM has a cohesive, thick, and compact matrix [16,17].

Junjie Wang et al. (2020) [18] explored the effects of initial curing temperatures and times on the microstructures, reaction products, and physical characteristics of GRAC (geopolymer recycled aggregate concrete) at varying ratios of fly ash to GGBS. With most fractures passing via recycled aggregate, the failure mechanism of GRAC was similar to that of OPC-based concrete. As the curing temperature rose, the toughness, elastic modulus, and compressive strength (CS) increased while the compression resistance dropped. Twelve to twenty-four hours was the ideal first curing period for GRAC. The geopolymer matrix grew denser and more compact with a more significant GGBS concentration, and the mechanical characteristics enhanced as the GGBS/fly ash ratio rose. Because of the higher Si and Al ions, geopolymer cement produced with an alkali solution has a denser C-A-S-H structure. After extended curing, its CS rises to 58.6 MPa from 20.4 MPa. The penetrability of chloride ions is decreased by the extended curing period. Even in extreme weather, the geopolymer reaction in GC may continue due to its strong resilience to weathering. Its potential for advancement in building applications is shown by the fact that, at a concentration of 4 M NaOH, the maximal CS is reached (Wei-Hao Lee et al., 2019) [19]. According to Jianhe Xie et al. (2019) [18], the mixture of GGBS and fly ash improves the mechanical performance and workability of the concrete. With the same W/B ratio, GRAC concrete may have a more considerable slump value than OPC concrete, and the GGBS component significantly impacts uniformity. Compared to other concrete, GRAC exhibits a significant improvement in its elastic modulus and a superior ability for energy dissipation. The modes of failure of GC change as the concentration of GGBS rises, and it is found that the geopolymer binder matrix is denser than the OPC matrix.

According to Min Yu et al. (2024) [20], geopolymer products underwent a phase transition at temperatures lower than 300°C, which reduced their strength. The GC and GPM specimens' residual CS

dropped as exposure temperature rise. Compared to GPM specimens devoid of steel fibre, GC specimens exhibited a greater residual CS. The remaining elastic modulus decreased more quickly than CS. The steel-fibered GPM specimen showed the highest rate of rise in peak strain as the exposure temperature rise. While fly ash-based GC mixes have similar qualities at all ages, at room temperature, GGBS blended FA-based mixtures offer better mechanical characteristics without heat curing. These materials are an affordable choice for building since they provide sustainability, financial savings, and environmental advantages (Abhilash et al. 2016) [21]. G. Murali (2023) [2] investigated the characteristics and microstructure of ultra-high-performance concrete (GUHPC) based on geopolymer to maximize its strength and ability to support loads for infrastructure. It was discovered that adding more SLF (silica fume) enhances fluidity, adding S.F. increases CS, and adding 30% SLF and slag increases tensile strength (TS). The study also showed that fly ash and dissolved GGBFS aid in polymerization.

Felix Kugler et al. (2022) [22] examined the synthesis of geopolymers using an alkaline activator solution, fly ash, and concrete debris. It examines whether concrete rubble is a suitable matrix material for geopolymerization and how increasing amounts affect the material's structures, setting response, and other characteristics. XRD analysis and I.R. spectroscopy reveal the geo-polymerization process, and all geopolymer batches exhibit appropriate CSs. The results indicate the possibility of creating fly ash-concrete rubble geopolymers with better qualities than traditional building materials, which would support the development of a decarbonized sector.

Firdous and Stephan (2019) [23] have reported that the reactivity of natural pozzolans in an alkaline media is influenced by their mineralogical and chemical composition. The degree of polymerization determines the mechanical characteristics of the resulting gel, whereas the dissolution of silicate and aluminate species rises with a decrease in silica modulus. Reduced polymerization and efflorescence caused by low silica modulus decreased CS. In terms of characteristics and economy, it is not advised to increase the silica modulus in order to get a greater CS. For naturally occurring pozzolan-based geopolymers, the selective dissolving approach is appropriate for estimating the volume of geopolymer product generated.

According to Gugulothu and Gunneswara (2020)[24], the GC is an environmentally friendly alternative OPC concrete, utilizing GGBS activated with sodium silicate solution. This study investigated the use of neutral-grade sodium silicate solution to mitigate the rapid setting behavior of GGBS, finding that it effectively increases setting time. The experimental program evaluated workability and CS for various solution/binder ratios and binder contents, achieving CSs up to 80 MPa and workability ranging from 80 to 110 mm. The results demonstrate that GC can be effectively activated under ambient curing conditions, making it suitable for construction applications with high-performance outcomes. Gugulothu Vikas and Gunneswara (2021) [25]. have examined the consistency, setting time, workability, and CS of GC. The findings show that GGBS-based GC, when activated with neutral grade water glass, has increased setting times and workability but higher CS as the slag percentage rises. FA-based GC exhibits a high slump but lower CS. The study concludes that geopolymer mixes with high FA content can be cured in ambient conditions, making them a viable alternative to conventional concrete.

This research is significant because it explores the viability of GC as a sustainable alternative to conventional concrete, which is crucial given the environmental impact of traditional cement production. Cement production is a major contributor to global CO<sub>2</sub> emissions, and finding alternatives that reduce greenhouse gas emissions is vital for addressing climate change. The present study used water glass as an alkali activator, while GGBS and FA were raw ingredients to make GC. Mechanical properties and microstructure analysis were done on the GC. The primary objective of the research was to investigate the physical properties of the different materials used in this study. To ascertain the mechanical properties of various GC grades. To analyze the GC microstructure using XRD, EDS, and SEM analysis.

## 2. Experimental Procedure

### 2.1 Binders

As binders, F.A. and GGBS were utilized; their specific gravities are 2.15 and 2.85, and their fineness is 360 and

400 m<sup>2</sup>/kg, respectively. Class F fly ash gathered from RAMAGUNDAM in Telangana is used in this project. Table 1 lists the chemical characteristics.

**Table 1. Chemical Composition of GGBS and FA**

| Sl. No. | Composition                    | Fly ash (% by mass) | GGBS (% by mass) |
|---------|--------------------------------|---------------------|------------------|
| 1       | SiO <sub>2</sub>               | 58.19               | 32.47            |
| 2       | Al <sub>2</sub> O <sub>3</sub> | 39.02               | 14.45            |
| 3       | CaO                            | 0.90                | 40.74            |
| 4       | MgO                            | 0.28                | 6.99             |
| 5       | K <sub>2</sub> O               | 0.88                | 0.29             |
| 6       | Na <sub>2</sub> O              | 0.88                | 0.16             |

### 2.2 Aggregates

Crushed granite stone readily accessible was utilized as a coarse aggregate with nominal sizes of 10 mm and 20 mm. In compliance with I.S. 383:2016[26] requirements, the fine aggregate was made using sand from neighbouring rivers. Table 2 assigns the aggregates' physical characteristics.

**Table 2. Fine aggregate characteristics**

| S. No. | Tests                             | Fine Aggregate | Coarse aggregate |
|--------|-----------------------------------|----------------|------------------|
| 1      | Fineness Modulus                  | 3.52           | 7.57             |
| 2      | Bulk density (kg/m <sup>3</sup> ) | 1.71           | 1.55             |
| 3      | Specific gravity                  | 2.64           | 2.72             |

### 2.3 Water Glass/ Alkali Activator

Water glass is a glassy substance that can be soluble in water. It is made of sodium oxide and silica. Other names for it include alkali silicate glass and sodium silicate glass. Water glass might be a smooth, syrupy liquid, or it can be hardened into lumps or powder. The chemical formula for water glass is Na<sub>2</sub>SiO<sub>3</sub>. In this instance, the symbol s stands for the modulus value of the water glass, which expresses the molar ratio of silicon dioxide to sodium oxide.

### 2.4 Mix Proportion

The mix design of GC was arrived at after several trials. Table 3, 4, and 5 displays the mix proportion for M25, M40 and M70 grade.

**Table 3. Mix Proportions of M70**

| Alkali Binder Ratio | GGBS (kg/m <sup>3</sup> ) | FlyAsh (kg/m <sup>3</sup> ) | 20mm (kg/m <sup>3</sup> ) | 10mm (kg/m <sup>3</sup> ) | R Sand (kg/m <sup>3</sup> ) | Liquid (kg/m <sup>3</sup> ) |
|---------------------|---------------------------|-----------------------------|---------------------------|---------------------------|-----------------------------|-----------------------------|
| 0.4                 | 480                       | 120                         | 515                       | 422                       | 623                         | 240                         |

|     |     |     |     |     |     |     |
|-----|-----|-----|-----|-----|-----|-----|
| 0.5 | 480 | 120 | 495 | 406 | 599 | 300 |
| 0.6 | 480 | 120 | 475 | 390 | 575 | 360 |
| 0.7 | 480 | 120 | 455 | 374 | 551 | 420 |

Table 4 Mix Proportions of M40

| Alkali Binder Ratio | GGBS (kg/m <sup>3</sup> ) | FlyAsh (kg/m <sup>3</sup> ) | 20mm (kg/m <sup>3</sup> ) | 10mm (kg/m <sup>3</sup> ) | R Sand (kg/m <sup>3</sup> ) | Liquid (kg/m <sup>3</sup> ) |
|---------------------|---------------------------|-----------------------------|---------------------------|---------------------------|-----------------------------|-----------------------------|
| 0.4                 | 270                       | 180                         | 585                       | 479                       | 706                         | 180                         |
| 0.5                 | 270                       | 180                         | 570                       | 467                       | 688                         | 225                         |
| 0.6                 | 270                       | 180                         | 555                       | 455                       | 670                         | 270                         |
| 0.7                 | 270                       | 180                         | 540                       | 443                       | 652                         | 315                         |

Table 5 Mix Proportions of M25

| Alkali Binder Ratio | GGBS (kg/m <sup>3</sup> ) | FlyAsh (kg/m <sup>3</sup> ) | 20mm (kg/m <sup>3</sup> ) | 10mm (kg/m <sup>3</sup> ) | R Sand (kg/m <sup>3</sup> ) | Liquid (kg/m <sup>3</sup> ) |
|---------------------|---------------------------|-----------------------------|---------------------------|---------------------------|-----------------------------|-----------------------------|
| 0.4                 | 165                       | 165                         | 642                       | 518                       | 776                         | 132                         |
| 0.5                 | 165                       | 165                         | 631                       | 509                       | 763                         | 165                         |
| 0.6                 | 165                       | 165                         | 620                       | 500                       | 750                         | 198                         |
| 0.7                 | 165                       | 165                         | 609                       | 491                       | 737                         | 231                         |

## 2.5 Mixing and Casting

GC was cast using the same technique as OPC concrete. In a mixing pan, dry conditions were first combined with coarse and fine aggregates for two minutes. Next, the binder was added, and the mixture was stirred for two more minutes. After adding the alkali liquid, the dry ingredients were blended for two more minutes. After that, the entire mixture was mixed for four minutes or until the mixture was homogenous. Following mixing, three layers of the fresh concrete were cast in moulds, and each layer was tamped for 35 blows. Figure 1 shows the mixing and casting of GC.



Figure 1 Mixing and casting of GC

## 3. Experimental Investigation

### 3.1. Slump Test

The workability of fresh GC was evaluated using slump test as per the guidelines given in IS: 1199-1959 (Reaffirmed in 2004)[26] with alkali/binder ratio of 0.4, 0.5, 0.6, 0.7 for grades M25, M40 and M70 respectively. The evaluation was done using water glass as the alkaline activator. The slump cone used for the test had a top diameter of 100 mm, a height of 300 mm and a base diameter of 200 mm.

### 3.2. Compressive Strength

According to IS 516: 2018[27], a CS test was performed on concrete cube specimens of 150 mm by 150 mm by 150 mm. The tests were conducted using a compression testing machine with a maximum capacity of 2000 kN. During the test, the load was applied at a constant rate of 14 MPa per minute. An experimental setup for assessing the cube's CS is illustrated in Figure 2.



Figure 2. Compressive Testing of Cube Specimen

### 3.3 Split Tensile Strength

The cylinders with a 30 cm height and dia. of 15 cm are used for testing strength by IS 5816-1970 [28] specifications. Following 7 and 28 days of curing, the test was performed. Lastly, the following formula was used to get the TS. The cylinder specimen was tested, as shown in Figure 3.



Figure 3 Split Tensile Testing of Cylinder Specimen

### 3.4. Flexural Strength

The test for flexural strength was conducted in compliance with the IS 516-2004 [28] test procedure. The specimens used were beams measuring 500 mm by 100 mm by 100 mm. Seven and twenty-eight days following the cure, the test was conducted.

## 4. Results and discussion

### 4.1. Slump Test

Fig. 4 presents the slump test results of the alkali/binder ratio of 0.4, 0.5, 0.6, and 0.7 for grades M25, M40, and M70. The workability gradually decreases as the grades M25, M40, and M70 increase for all alkali/binder ratios of 0.4, 0.5, 0.6, and 0.7, as shown in Figure 4. It was also observed that, for alkali/binder ratio increases, the slump value is gradually increased from 0.4, 0.5, 0.6, 0.7. In the case of an alkali/binder ratio of 0.4, the slump value for grades M25, M40, and M70 is 70mm, 60mm, and 40mm, respectively. For an alkali/binder ratio of 0.5, the slump value for grades M25, M40, and M70 is 100mm, 90mm, and 70mm. For an alkali/binder ratio of 0.6, the slump value is 120 mm, 110mm, and 90mm, respectively. The slump value of alkaline-activated sodium silicate-based GC tends to decrease as the grade of GC increases (from M25 to M40 to M70), primarily due to increased binder content. Generally,

higher grade mixes typically contain more binder materials (fly ash and GGBS), which increases alkaline liquid demand and reduces workability.

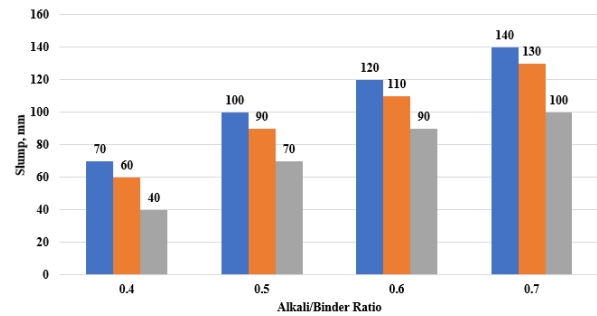


Figure. 4 Slump Values of alkali/binder ratio of 0.4, 0.5, 0.6, and 0.7 for M25, M40, and M70 grades

The study used higher GGBS percentages for higher grades for M25, M40, and M70, which tend to reduce workability. Higher grade mixes may have increased reactivity between the binder materials and alkaline activator, leading to faster setting and reduced workability. Higher strength mixes often have optimized particle packing, which can reduce the amount of free water available for workability. The study found that increasing the alkali-to-binder ratio from 0.4 to 0.7 generally increased slump values across all grades, likely due to increased liquid content improving workability [25,26]. However, the trend of decreasing slump with increasing grade was maintained even at higher alkali-to-binder ratios.

### 4.2. Compressive strength

The CS of GC at 7 and 28 days with different combinations of alkaline binder ratios are shown in Figure 5. Among alkali-to-binder ratios ratios 0.4, 0.5, 0.6, and 0.7, the alkali-to-binder ratios of 0.6 shows the highest CS of GC for M25, M40, and M70 grades. The alkali-to-binder ratios of 0.4 and 0.5 show the lowest CS at 7 and 28 days with different grades of GC, as shown in Figure 5. This may be due to lower alkali-to-binder ratios such as 0.4 and 0.5, or there may be insufficient activator to fully react with the binder, resulting in incomplete geo-polymerisation and lower strength. The strength decreases after increasing the alkali-to-binder ratios beyond 0.6, excess activator may lead to the formation of weaker structures or unreacted material, negatively impacting the overall strength of the concrete. For 28 days of ambient curing, the highest CS of 28.3, 51.7 & 72.8 N/mm<sup>2</sup> was achieved by M25, M40 & M70 grades, respectively, with an alkaline to-binder ratio of 0.6.

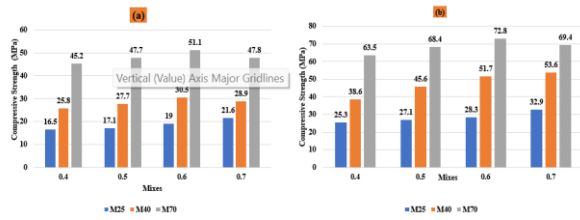


Figure 5: Compressive strength of 0.4, 0.5, 0.6, and 0.7 for M25, M40, and M70 grades GC at (a) 7 days, (b) 28 days

### 4.3 Split tensile strength

Figure 6 illustrates the A/B ratio in a blend of different grades of GC. For A/B ratios of 0.4, 0.5, and 0.6, the TS of M25, M40, and M70 grades of GC progressively increases. However, once the A/B ratio reaches 0.7, there is a significant drop in TS, as depicted in Figure 6. The GC with an A/B ratio of 0.6 demonstrated TS values of 2.25, 4.60, and 6.73 N/mm<sup>2</sup> for M25, M40, and M70 grades of GC after 28 days of curing, respectively.

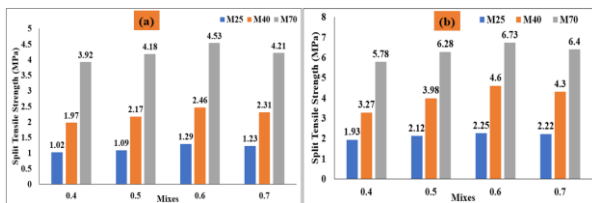


Figure 6. Split Tensile strength of 0.4, 0.5, 0.6, and 0.7 for M25, M40, and M70 grades GC at (a) 7 days, (b) 28 days

### 4.4 Flexural strength

Figure 7 illustrates the flexural strengths for concrete grades M25, M40, and M70. At 28 days, with an alkali to binder ratio of 0.6, the flexural strengths for M25, M40, and M70 grades of GC are 2.25, 4.60, and 6.73 N/mm<sup>2</sup>, respectively. Similar to the behaviour of the geopolymer composite in split tensile and CS, the FS also rises with an increased alkali to binder ratio across different GC grades. The most notable strength improvements of approximately 13.9%, 37.02%, and 15.5% are recorded at 28 days for the M25, M40, and M70 mixes with an A/B ratio of 0.6 compared to a 0.4 A/B ratio. Figure 7 shows the variation in FS in GC.

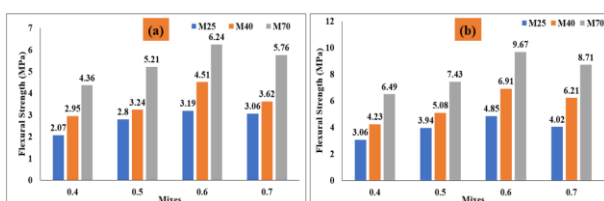


Figure 7 Flexural strength of GC

### 4.5. Empirical Relations

A comparative analysis was conducted between CS and TS, and between CS and FS for M25, M40, and M70 grade mixes at an alkali-to-binder ratio of 0.6 after 28 days, as illustrated in Figures 8(a) and 8(b). The results indicated a strong correlation, with the coefficient of determination ( $R^2$ ) for the 28-day GC specimens being approximately equal to 1. This suggests an excellent exponential relationship between the compared strength parameters at the given alkali-to-binder ratio.

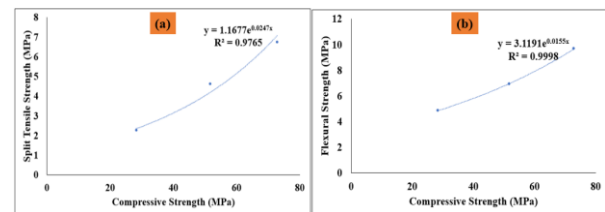


Figure 8. Correlation alkali-to-binder ratio at 0.6 for M25, M40 and M70 grade GC (a) CS Vs TS of GC (b) CS Vs FS of GC

### 4.6 Microstructure analysis

#### 4.6.1 SEM

A ZEISS microscope was used to study the samples under a microscope. Samples with dimensions as tiny as 1 nanometre can be seen with this ZEISS microscope. On unheated M25, M40, and M70 grade GC, SEM and EDS investigations are carried out to examine the microstructural behaviour of GC. For SEM and EDS examination, a tiny sample of the concrete was removed from its center. In order to use field emission SEM to photograph the smallest topographical components of the sample surface, images are obtained in the SEM imaging mode of unheated samples.

The fractured surfaces of specimens undergoing CS tests are examined using scanning electron microscopy. Figures 9 to 11 illustrate the microstructure of geopolymer samples of grades M25, M40, and M70 for A/B of 0.6. The microstructure reveals a strong bond between the GGBS-based GC and the reacted FA at the interface. The M70 grade material is denser and less porous, as seen in SEM images. Consequently, the M70 grade exhibits higher CS compared to the M25 and M40 grades. There are no cracks due to the polymerized binder. The micrographs of the different concrete grades appear denser because of increased gel formation. Therefore, GC demonstrates excellent CS.

The strength of the mixture results from the products formed when different particles interact with water glass solutions. Additionally, all M25, M40, and M70 grade GC shows a fully reacted matrix between the gel and the aggregate, as shown in Figures 9 to 11, indicating strong cohesion between the binder and aggregate.

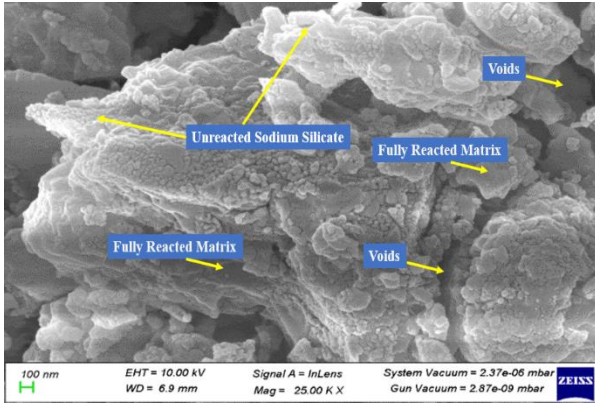


Figure 9 SEM images of M25 grade GC

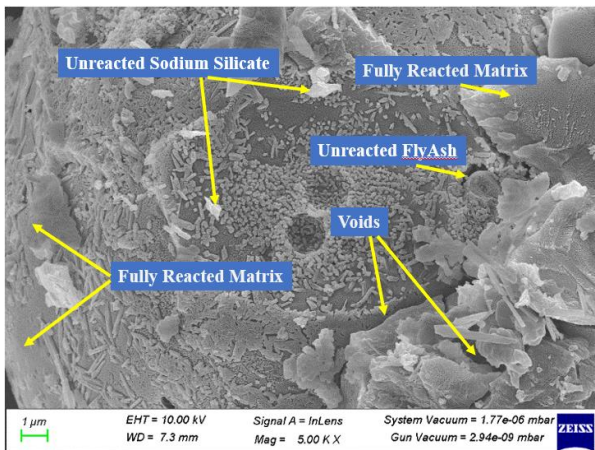


Figure 10 SEM images of M40 grade GC

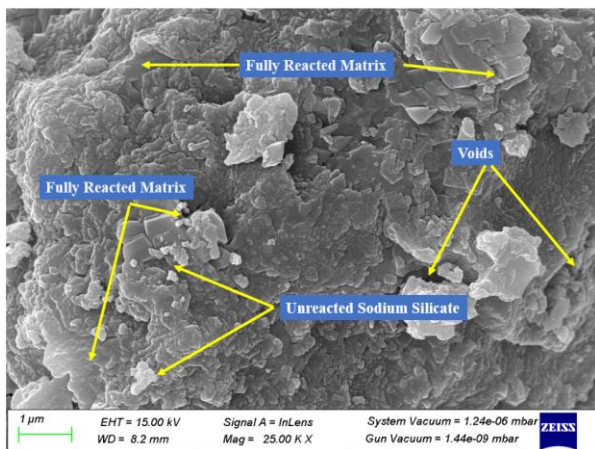


Figure 11 SEM images of M70 grade GC

The EDS results will reveal the atomic and weight percentages of the different elements presented in Table 6. Table 6 illustrates the weight percentages for the M25, M40, and M70 grade components for A/B of 0.6 at 28 days of ambient curing. This analysis is performed alongside SEM analysis, which offers a quantitative assessment of the elements within the geopolymer. Compositional data can be extracted from the EDS findings.

Table 6 EDS analysis of M25, M40 and M70 grades GC for alkali to binder ratio of 0.6

| Element | M25        | M40        | M70        |
|---------|------------|------------|------------|
|         | Weight (%) | Weight (%) | Weight (%) |
| Mg      | 1.3        | 0.7        | 0.7        |
| Al      | 14.2       | 4.1        | 2.9        |
| Si      | 41.8       | 14.4       | 12.2       |
| K       | 0.00       | 1.2        | 1.9        |
| Ca      | 25.1       | 64.0       | 70.4       |
| Fe      | 5.1        | 10.4       | 4.8        |
| Cu      | 1.10       | 0.2        | 2.3        |
| Zn      | 11.3       | 5.0        | 4.9        |

The weight and atomic percentages from the EDS analysis of materials with varying molarities at specific locations are depicted in Figures 12 to 14. Both minor and major component concentrations can be identified. Alumina and silica play a crucial role in enhancing GC strength, indicating an increase in Si and Al. The M25 and M40 grades contain lower Si and Al components compared to M70. However, the addition of silica and alumina oxides may lead to a significant improvement in CS.

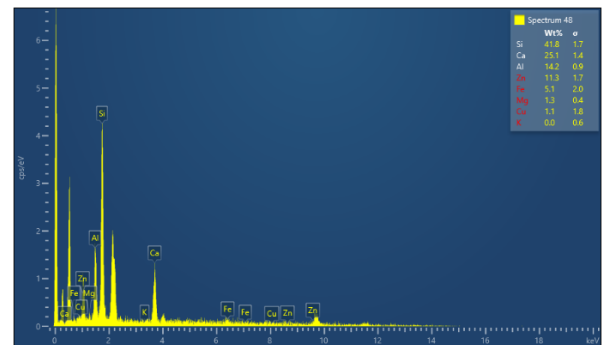


Figure 12: EDS analysis of GC concrete of M25 grade

#### 4.6.2 EDS

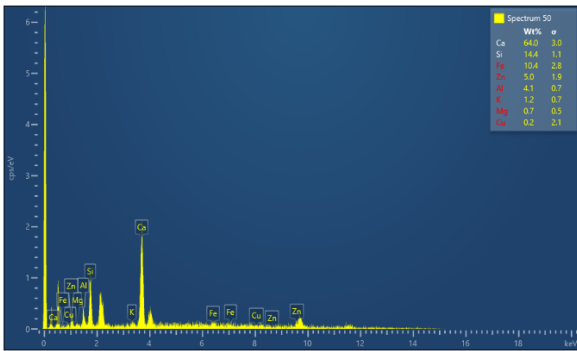


Figure 13: EDS analysis of GC concrete of M40 grade

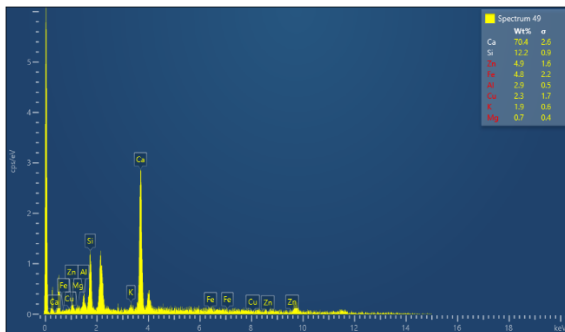


Figure 14: EDS analysis of GC concrete of M70 grade

#### 4.6.3 The Analysis of X-Ray Diffraction (XRD)

The Xpert High Score software is utilized to analyze XRD analysis, with Figures 15 to 17 showing distinct peaks corresponding to various elements in the samples. The vertical axis represents peak intensity, while the horizontal axis shows the  $2\theta$  angle. The software analyzes the five phases of quartz, ferrous, magnesium, calcium oxide, and C-S-H, represented in blue, aqua, lime, grey, and maroon. Elements from the periodic table, which display chemical properties, can be selected for analysis. Each phase is designated by a specific color, as illustrated in Figure 15, which shows the peak values of elements found in M25 grade GC, while Figures 16 and 17 display the XRD peaks for M40 and M70 grade concrete.

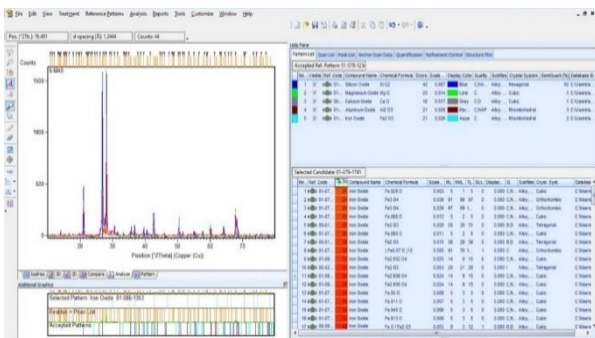


Figure 15 XRD ranges of GC of M25 grade

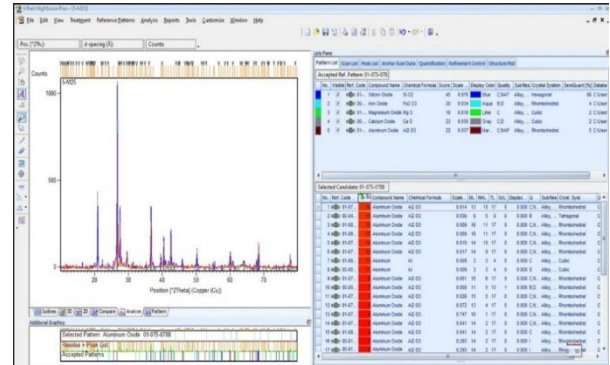


Figure 16 XRD ranges of GC of M40 grade

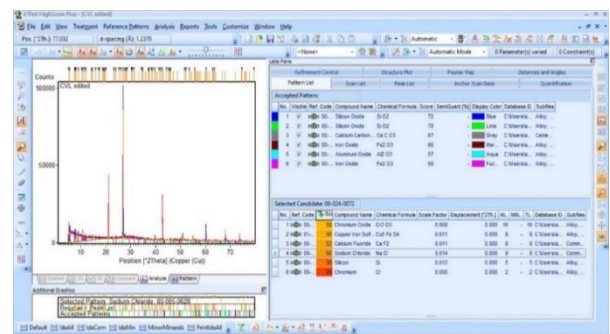


Figure 17 XRD ranges of GC of M70 grade.

## 5. Conclusions

The strength characteristics of various grades of GC with varying A/B ratios and the microstructure analysis of multiple grades of GC under SEM, EDS, and XRD were investigated through experiments. It is possible to reach the following conclusions. As the alkali-to-binder ratio rose from 0.4% to 0.6%, the mechanical strength parameters of the GC composite improved for all mixtures. According to the results of the FS, TS, CS tests, the mechanical performance of FA-GGBS GC is enhanced by using higher concrete grades and increasing the water glass solution to binder ratio by up to 0.6. The analysis of microstructure results indicates that the microscopy images correlate with the CS of the GC specimen. The crystalline phase of FA-GGBS-based GC is identified by the peaks of quartz in XRD spectra. Increasing the water glass content increases CS, making the concrete dense. In EDX analysis, it is found that the rise in Si in M25, M40 & M70 grades leads to high strength and also improved the rate of geo polymerization; EDX results reveal that, with the addition of water glass, potassium oxide is increased, which yields in TS, FS, and CS.

## References

- [1] B.V. Prasad, N. Anand, B. Kanagaraj, T. Kiran, M.Z. Naser, P.D. Arumairaj, D. Andrushia, Investigation on residual bond strength and microstructure characteristics of fiber-

- reinforced geopolymer concrete at elevated temperature, *Case Stud. Constr. Mater.* 19 (2023) e02526. <https://doi.org/10.1016/j.cscm.2023.e02526>.
- [2] G. Murali, Recent research in mechanical properties of geopolymer-based ultra-high-performance concrete: A review, *Def. Technol.* 32 (2024) 67–88. <https://doi.org/10.1016/j.dt.2023.07.003>.
- [3] Vijaya Prasad B, A.P. Paul Daniel, A. N, S.K. Yadav, Strength and microstructure behaviour of high calcium fly ash based sustainable geopolymer concrete, *J. Eng. Des. Technol.* 20 (2021) 436–454. <https://doi.org/10.1108/JEDT-03-2021-0178>.
- [4] C. Zhao, Z. Li, S. Peng, J. Liu, Q. Wu, X. Xu, State-of-the-art review of geopolymer concrete carbonation: From impact analysis to model establishment, *Case Stud. Constr. Mater.* 20 (2024) e03124. <https://doi.org/10.1016/j.cscm.2024.e03124>.
- [5] B. Vijaya Prasad, A.K. P, N. Anand, P.D. Arumairaj, T. Dhilip, M.S. Kumar, Experimental Investigation on Fresh and Hardened Properties of High Calcium Flyash Based Geopolymer Concrete, *Mater. Sci. Forum.* 1048 (2022) 412–419.
- [6] V.P. Burle, T. Kiran, N. Anand, D. Andrushia, Post-fire investigation on the mechanical properties and physical characteristics of fibre-reinforced geopolymer concrete, *J. Struct. Fire Eng.* 2030 (2023). <https://doi.org/10.1108/JSFE-01-2023-0016>.
- [7] Vijaya Prasad, Arumairaj., Recent Advancements in Geopolymer Concrete using Class-F and Class-C Fly Ash, *Int. J. Innov. Technol. Explor. Eng.* 8 (2019) 5879–5884. <https://doi.org/10.35940/ijitee.l2599.1081219>.
- [8] V. Vinay Kumar, V. Bhikshma, B. Vijaya Prasad, Study on fresh and mechanical properties for different grades of geopolymer concrete with recycled coarse aggregate, *Mater. Today Proc.* 60 (2022) 708–714. <https://doi.org/10.1016/J.MATPR.2022.02.326>.
- [9] J. Davidovits, *Properties Of Geopolymer Cements*, n.d. [www.geopolymer.org](http://www.geopolymer.org).
- [10] B. V Rangan, B.V. Rangan, P. Fieaust, C. Faci, FLY ASH-BASED GEOPOLYMER CONCRETE, 2008.
- [11] B. Vijaya Prasad, N. Anand, P.D. Arumairaj, M.S. Kumar, T. Dhilip, G. Srikanth, Studies on mechanical properties of high calcium fly ash based sustainable geopolymer concrete, in: *J. Phys. Conf. Ser.*, IOP Publishing Ltd, 2021. <https://doi.org/10.1088/1742-6596/2070/1/012184>.
- [12] V.V. Kumar, V. Bhikshma, B.V. Prasad, Investigation On High-Strength Geopolymer Concrete with UFGGBS and Recycled Coarse Aggregate, *Libr. Prog. Int.* 44 (2024) 695–706.
- [13] B. Vijaya Prasad, N. Anand, T. Kiran, G. Jayakumar, A. Sohliya, S. Ebenezer, Influence of fibers on fresh properties and compressive strength of geo-polymer concrete, *Mater. Today Proc.* 57 (2022) 2355–2363. <https://doi.org/10.1016/j.matpr.2022.01.426>.
- [14] K. Pasupathy, M. Berndt, J. Sanjayan, P. Rajeev, D.S. Cheema, Durability performance of precast fly ash-based geopolymer concrete under atmospheric exposure conditions, *J. Mater. Civ. Eng.* 30 (2018) 1–9. [https://doi.org/10.1061/\(ASCE\)MT.1943-5533.0002165](https://doi.org/10.1061/(ASCE)MT.1943-5533.0002165).
- [15] M.B. Jaji, G.P.A.G. van Zijl, A.J. Babafemi, Durability and pore structure of metakaolin-based 3D printed geopolymer concrete, *Constr. Build. Mater.* 422 (2024) 135847. <https://doi.org/10.1016/j.conbuildmat.2024.135847>.
- [16] I.Y. Hakeem, O. Zaid, M.M. Arbili, M. Alyami, A. Alhamami, M. Alharthai, A state-of-the-art review of the physical and durability characteristics and microstructure behavior of ultra-high-performance geopolymer concrete, *Heliyon.* 10 (2024) e24263. <https://doi.org/10.1016/j.heliyon.2024.e24263>.
- [17] K. Pasupathy, M. Berndt, J. Sanjayan, P. Rajeev, D.S. Cheema, Durability of low-calcium fly ash based geopolymer concrete culvert in a saline environment, *Cem. Concr. Res.* 100 (2017) 297–310. <https://doi.org/10.1016/j.cemconres.2017.07.010>.
- [18] J. Xie, J. Wang, R. Rao, C. Wang, C. Fang, Effects of combined usage of GGBS and fly ash on workability and mechanical properties of alkali activated geopolymer concrete with recycled aggregate, Elsevier Ltd, 2019. <https://doi.org/10.1016/j.composites.2018.11.067>.
- [19] W.H. Lee, J.H. Wang, Y.C. Ding, T.W. Cheng, A study on the characteristics and microstructures of GGBS/FA based geopolymer paste and concrete, *Constr. Build. Mater.* 211 (2019) 807–813. <https://doi.org/10.1016/j.conbuildmat.2019.03.291>.
- [20] M. Yu, T. Wang, Y. Chi, D. Li, L. yuan Li, F. Shi, Residual mechanical properties of GGBS-FA-SF blended geopolymer concrete after exposed to elevated temperatures, *Constr. Build. Mater.* 411 (2024) 134378. <https://doi.org/10.1016/j.conbuildmat.2023.134378>.
- [21] P. Abhilash, C. Sashidhar, I. V. Ramana Reddy, Strength properties of fly ash and GGBS based

- geo-polymer concrete, *Int. J. ChemTech Res.* 9 (2016) 350–356.  
<https://doi.org/10.34218/ijciet.11.6.2020.012>.
- [22] F. Kugler, J. Karrer, W. Krcmar, U. Teipel, Setting behavior and mechanical properties of concrete rubble fly ash geopolymers, *Open Ceram.* 11 (2022).  
<https://doi.org/10.1016/j.oceram.2022.100286>
- [23] R. Firdous, D. Stephan, Effect of silica modulus on the geopolymerization activity of natural pozzolans, *Constr. Build. Mater.* 219 (2019) 31–43.  
<https://doi.org/10.1016/j.conbuildmat.2019.05.161>.
- [24] V. Gugulothu, T.D. Gunneswara Rao, Effect of Binder Content and Solution/Binder Ratio on Alkali-Activated Slag Concrete Activated with Neutral Grade Water Glass, *Arab. J. Sci. Eng.* 45 (2020) 8187–8197.  
<https://doi.org/10.1007/s13369-020-04666-5>.
- [25] G. Vikas, T.D.G. Rao, Setting Time, Workability and Strength Properties of Alkali Activated Fly Ash and Slag Based Geopolymer Concrete Activated with High Silica Modulus Water Glass, *Iran. J. Sci. Technol. - Trans. Civ. Eng.* 45 (2021) 1483–1492. <https://doi.org/10.1007/s40996-021-00598-8>.
- [26] IS: 383, Specification for Coarse and Fine Aggregates From Natural Sources for Concrete, 1970.
- [27] IS: 516, Method of Tests for Strength of Concrete -specifications, New Delhi, India., 2004.
- [28] IS: 5816, Method of Test Splitting Tensile Strength of Concrete, in: Indian Stand. Code, New Delhi, 1999.